

## Experimental and Theoretical Study of 4-Methylaminoantipyrine with Divalent Metal Ions

Farah M. Ibrahim

Department of Chemistry, college of Science, Al-Nahrain University, Baghdad-Iraq.

Corresponding author: farahtaha2016@gmail.com

### Abstract

$\text{Co}^{2+}$ ,  $\text{Ni}^{2+}$ ,  $\text{Cu}^{2+}$  complexes with 4-methylaminoantipyrine (MAP) were synthesis and characterized by IR, UV-Vis., thermal analysis, CHNO-S analysis, magnetic susceptibility, conductivity measurements and this work includes a theoretical study of MAP complexes where it was done by the program of hyperchem8.0.7 using semi-empirical calculations. The PM3 method at 298 K used to calculate geometric properties, binding energy ( $\Delta E_b$ ), heat of formation ( $\Delta H^{\circ}_f$ ), total energy ( $\Delta E_{\text{tot}}$ ), ultraviolet and vibrational data of the MAP complexes. The comparing of experimental data with theoretical data gave good results, so the square planar geometry suggested for complexes. [DOI: [10.22401/JNUS.21.3.08](https://doi.org/10.22401/JNUS.21.3.08)]

Keywords: 4-methylaminoantipyrine, divalent metal ions, thermal analysis.

### Introduction

Antipyrine, aminopyrine and 4-methylaminoantipyrine compounds are used as analgesic, anti-inflammatory, antipyretic and anticancer drugs [1-4]. N-heterocyclic inhibition against pathogenic bacteria and fungi [5]. 4-methylaminoantipyrine and 4-aminoantipyrine are strong inhibitors of cyclooxygenase in the treatment of inflammatory pain [6-7]. 4-aminoantipyrine and its derivatives characterized by  $^1\text{H-NMR}$ , single-crystal X-ray diffraction and FTIR techniques, the theoretical vibration frequencies show good result with the experimental vibration frequencies data [8]. New derivatives of 4-aminoantipyrin have anti-breast cancer activity due to pyrazole, pyrrole and pyrimidine moieties were synthesis and characterized by elemental analysis and  $^{13}\text{C}$ ,  $^1\text{H}$  NMR, IR spectral [9]. Schiff bases derived from 4-aminophenazone were prepared and the structure of compounds investigated FT-IR, NMR, Mass studies, elemental analysis and screened to be antibacterial active agents[10-12]. 4-aminoantipyrine used as an inhibitor for the corrosion of mild steel in 0.5 M sulphuric acid solution, thermodynamics of adsorption were calculated. Quantum chemical calculations was calculate the electronic properties to expect the inhibitive effect of the compound [13]. The aim of work is prepared and characterized complexes of compound has pharmacology applications and compared

these data with computational calculation using Hyperchem 8.0.7 program to suggest the accurate structure of MAP complexes that which proposed the square planar geometry finally.

### Experimental

#### Instrumentation

Infrared spectra of (MAP) complexes measured by ALPHA FTIR spectrophotometer. Shimadzu UV-Vis 160A spectrophotometer were used for UV-Visible spectra of (MAP) complexes. Shimadzu 680 cc-flame measured the metal ion percent. CHNS-O analysis was carried out on EURO EA elemental analyzer. Thermal analyses (TG-DTG) were gained on a LINSEIS (STA PT-1000). Johnson Matthey's magnetic susceptibility balance can be used for paramagnetic and diamagnetic materials. Molar conductivity measurements carried by corning conductivity meter 220. Melting points of ligand and its complexes were measured by Gallenkamp M.F.B. 600.01 apparatus.

#### Preparation of MAP complexes

The divalent complexes were prepared by mixing aqueous solution(10ml) of metal salts ( $\text{CuSO}_4 \cdot 5\text{H}_2\text{O}$ ,  $\text{CoCl}_2 \cdot 2\text{H}_2\text{O}$  and  $\text{NiSO}_4 \cdot 6\text{H}_2\text{O}$ ) with aqueous solution(10ml) of MAP 1:2 (metal: ligand) mole ratio and refluxed for 12 hours. A colored precipitate was formed at room temperature, filtered and washed with distilled water then dried in oven at  $50^\circ\text{C}$ .

**Table (1)**  
**Some characterization data of MAP and metal complexes.**

Compound	Conductivity, DMF solvent $\mu\text{s}/\text{cm}$	Melting Point, $^{\circ}\text{C}$ colour	Found% (Calculate)%					
			C	H	O	N	S	Metal
MAP	-	White 110	66.30 (66.36)	6.90 (6.91)	7.35 (7.37)	19.30 (19.35)	-	-
CoMAP	146	Light pink 119-121	51.00 (51.08)	5.30 (5.32)	5.60 (5.67)	14.80 (14.89)	-	10.43 (10.45)
NiMAP	78	Light green 120-122	48.90 (48.92)	5.04 (5.09)	16.26 (16.31)	14.20 (14.27)	5.40 (5.43)	9.95 (9.97)
CuMAP	85	Light green 122-124	48.50 (48.52)	5.00 (5.05)	16.12 (16.17)	14.10 (14.15)	5.30 (5.39)	10.68 (10.70)

### IR Spectra

IR of MAP: A stretching vibration band at ( $3319.77\text{ cm}^{-1}$ ), ( $1652.34\text{ cm}^{-1}$ ), ( $3108.6\text{ cm}^{-1}$ ), ( $1610.09\text{--}1560.53\text{ cm}^{-1}$ ), ( $2877.09\text{ cm}^{-1}$ ), ( $2707.86\text{ cm}^{-1}$ ), ( $2793.51\text{ cm}^{-1}$ ), that corresponds to (NH), (C=O), (CH aromatic), (C=C aromatic), (CH asymmetric), (CH asymmetric), (CH symmetric) groups, respectively and bending vibration band at

( $1367.93\text{ cm}^{-1}$ ), ( $1435.68\text{ cm}^{-1}$ ), ( $1505.33\text{ cm}^{-1}$ ) that corresponds to (CH symmetric), (CH asymmetric), (NH) groups, respectively [8,14]. Coordination of the  $\pi$  electrons C=O reduces the double bond character of the C-O bond causing absorption at lower wave number, also the donor amino group shift due to the complexation with metal ion, see Fig.(1).

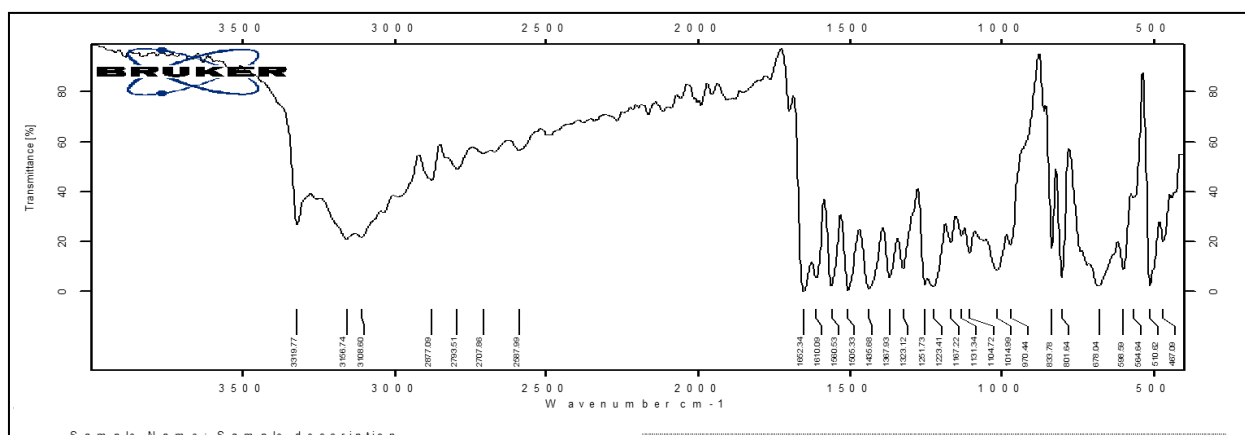


**Fig.(1): IR spectrum of MAP.**

Experimental IR of CoMAP: A stretching vibration band at ( $3332.75\text{ cm}^{-1}$ ), ( $1634.65\text{ cm}^{-1}$ ) that corresponds to (NH), (C=O) groups, respectively [15], see Fig.(2) and Table (2).

**Table(2)**  
**Experimental and Theoretical stretching vibration band for CoMAP ( $\text{cm}^{-1}$ ).**

Compound	Frequency		Intensity	
	Theoretical	Experimental		
CoMAP	NH (amine group)	3329	3332.75	100.00
	C=O	1639	1634.65	80.28
	C-H ( aromatic ring)	3003	3010	81.88
	C-H (aliphatic)	2900	2897.6	81.36
	C=C( aromatic ring)	1512	1510.34	163.13

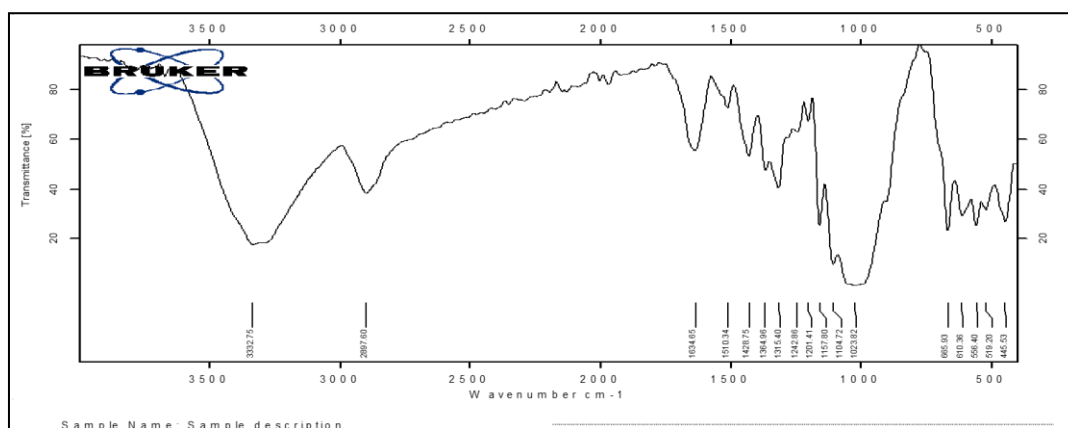


**Fig.(2): IR spectrum of CoMAP.**

Experimental IR of NiMAP compound: A stretching vibration band at ( $3331.06\text{ cm}^{-1}$ ), ( $1646.98\text{ cm}^{-1}$ ) that corresponds to (NH), (C=O) groups stretching vibrations, respectively [15], see Fig.(3) and Table (3).

**Table(3)**

**Experimental and Theoretical stretching vibration band for NiMAP ( $\text{cm}^{-1}$ ).**

Compound	Frequency	Intensity		
		Theoretical	experimental	
NiMAP	NH (amine group)	3340	3331.06	88.00
	C=O	1648	1646.98	81.32
	C-H (aromatic ring)	3003	3000	79.88
	C-H (aliphatic)	2895	2942.52	82.31
			2890.09	
	C=C (aromatic ring)	1512	1513.56	149.22

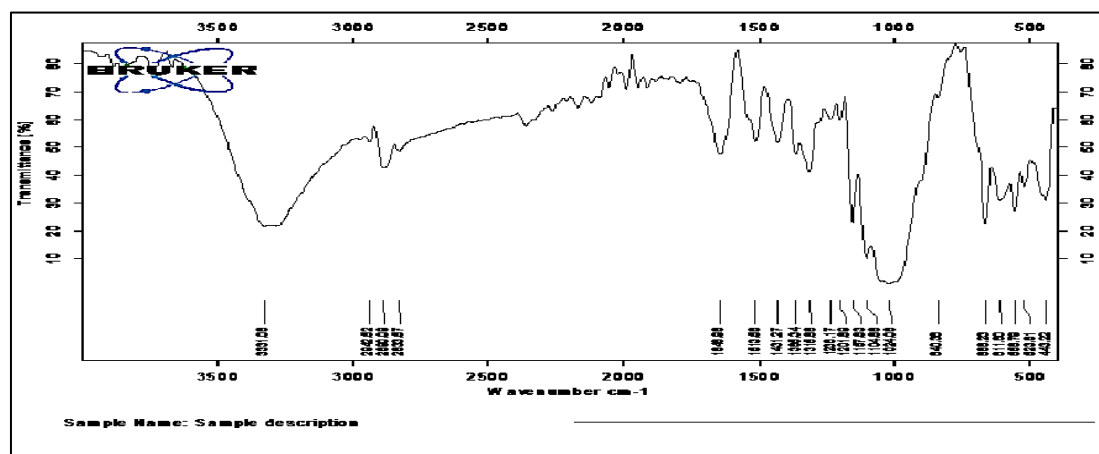


**Fig.(3): IR spectrum of NiMAP.**

Experimental IR of CuMAP compound: A stretching vibration band at ( $3282.23\text{ cm}^{-1}$ ), ( $1640.79\text{ cm}^{-1}$ ) that corresponds to (NH), (C=O) groups, respectively [16], see Fig.(4) and Table (4).

**Table(4)**  
**Experimental and Theoretical stretching vibration band for CuMAP ( $\text{cm}^{-1}$ ).**

Compound	Frequency		Intensity	
		Theoretical		experimental
CuMAP	NH (amine group)	3268	3282.23	88.00
	C=O	1645	1640.79	76.24
	C-H ( aromatic ring)	3003	3000.0	83.82
	C-H (aliphatic)	2877	2895.89 2959.88	80.30
	C=C( aromatic ring)	1508	1550.99-1502.0	89.47

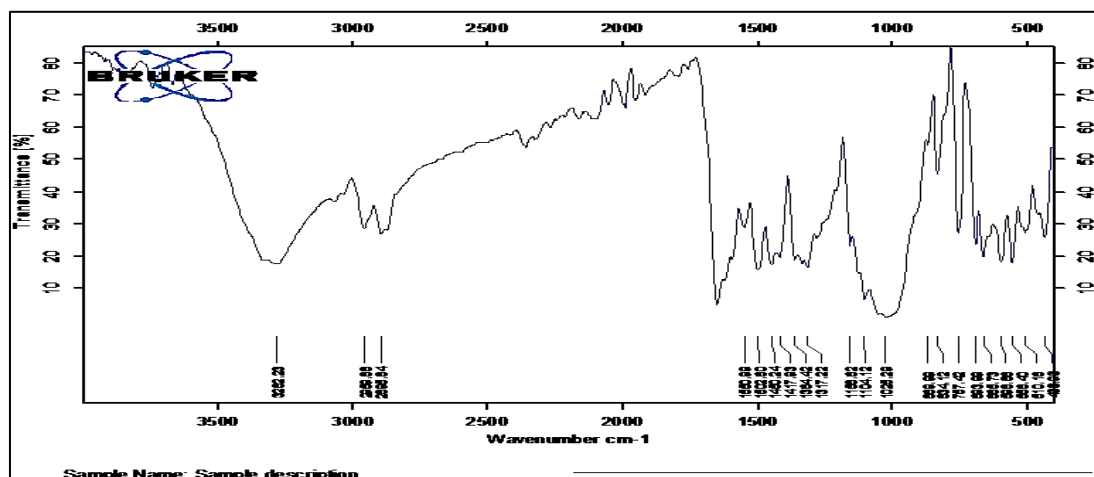


**Fig.(4): IR spectrum of CuMAP.**

### Ultraviolet-Visible spectroscopy and magnetic susceptibility

MAP spectrum showed bands at (216, 234, 266) nm were for  $\pi \rightarrow \pi^*$  electronic transition and at (305) nm for  $n \rightarrow \pi^*$  transition. Co MAP complex showed a band at 511 nm which is assigned to ( $^1A_{1g} \rightarrow ^1B_{1g}$ ) transition. NiMAP complex have bands at 630nm assigned to ( $^1A_{1g} \rightarrow ^1B_{1g}$ ) transition, CuMAP showed band at 559nm assigned to  $^2B_{1g} \rightarrow ^2A_{1g}$  transition, so square planar geometry were suggested for  $\text{Co}^{2+}$ ,  $\text{Ni}^{2+}$  and  $\text{Cu}^{2+}$  complexes [12].

**Table(5)**  
**Comparison of experimental and theoretical ultraviolet for complexes and  $\mu_{\text{eff}}$ .**

Compound	Experimental	Theoretical	$\mu_{\text{eff}}$ .B.M.	
CoMAP	$\pi \rightarrow \pi^*$ (nm)	240.0	245	2.5
	$n \rightarrow \pi^*$ (nm)	342.0,397	321	-
NiMAP	$\pi \rightarrow \pi^*$ (nm)	236	272	zero
	$n \rightarrow \pi^*$ (nm)	330	310	-
CuMAP	$\pi \rightarrow \pi^*$ (nm)	260	257	1.94
	$n \rightarrow \pi^*$ (nm)	281	277	-

### Thermal analysis of metal complexes

The thermo-gravimetry analysis help to investigated the structure of complexes, first loss of  $[\text{CoC}_{24}\text{H}_{30}\text{N}_6\text{O}_2\text{Cl}_2]$  gave  $[\text{CoC}_4\text{H}_2\text{N}_6]$  at 279-340C, the other loss at 380-500°C for elimination ( $\text{N}_4\text{C}_4\text{H}_2$ ) and remain  $[\text{CoN}_2]$ .  $[\text{NiC}_{24}\text{H}_{30}\text{N}_6\text{O}_6\text{S}]$  complex decomposes between 130-320 °C to form  $[\text{NiC}_2\text{N}_4\text{O}_6\text{S}]$  due to the elimination part ( $\text{C}_{22}\text{H}_{30}$ ) and the second loss is ( $\text{N}_4\text{C}_2\text{O}_3\text{S}$ ) between 390-560 °C to residue  $[\text{NiO}]$ , [17].  $[\text{CuC}_{24}\text{H}_{30}\text{N}_6\text{O}_6\text{S}]$  complex is assigned to the elimination of ( $\text{C}_{18}\text{H}_{22}\text{O}_2\text{N}_4$ ), the other loss of  $[\text{CuC}_6\text{H}_8\text{N}_2\text{O}_4\text{S}]$  is ( $\text{C}_4\text{H}_8\text{N}_4\text{O}_3\text{S}$ ) between 330-490 °C to remain  $[\text{CuO}]$ .

### Theoretical Study

Program hyperchem-8.0.7 was used for calculations of the heat of formation ( $\Delta H_f^\circ$ ), and binding energy ( $\Delta E_b$ ) for MAP complexes were calculated by the semi-empirical and molecular mechanics Table (6). Also, PM3 was used to evaluate the vibrational spectra of MAP complexes. It has been found that these obtained frequencies agree well with the experimental results Table (2-4), HOMO, LUMO and electrostatic potential as shown in Fig.(8), Bond length and bond angle measurements for the MAP complexes was calculated Tables (7-12) Optimization geometry of MAP complexes Figures (5-7) was obtained the PM3 method.

*Table(6)*  
*Conformation energetic (in KJ. mol<sup>-1</sup>), HOMO and LUMO energetic Dipole moment.*

Compd. No.	$\Delta E_{\text{tot}}$ kJ/mol	$\Delta H_f^\circ$ kJ/mol	$\Delta E_b$ kJ/mol	$E_{\text{HOMO}}$ eV	$E_{\text{LUMO}}$ eV	Dipole moment (Debye)
CoMAP	-611750.464	-1255.660	-29615.774	- 8.147772	- 2.0694	3.4965
NiMAP	-697298.57824	-2880.4329	-25859.295	-6.07491	-1.80383	10.2390
CuMAP	-722855.705	-1103.278	-30840.556	- 8.523952	- 0.3874507	8.7554

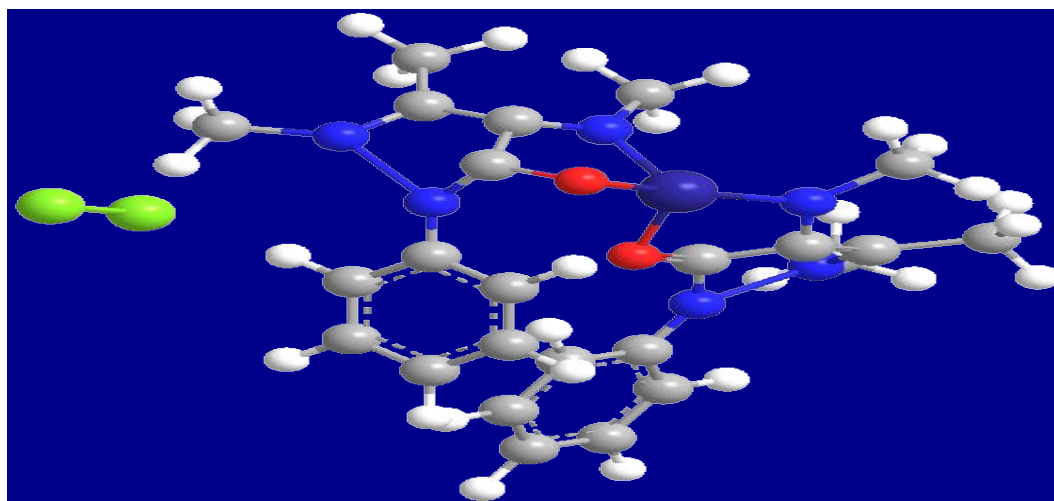


*Fig.(5): Optimized geometric for CoMAP.*

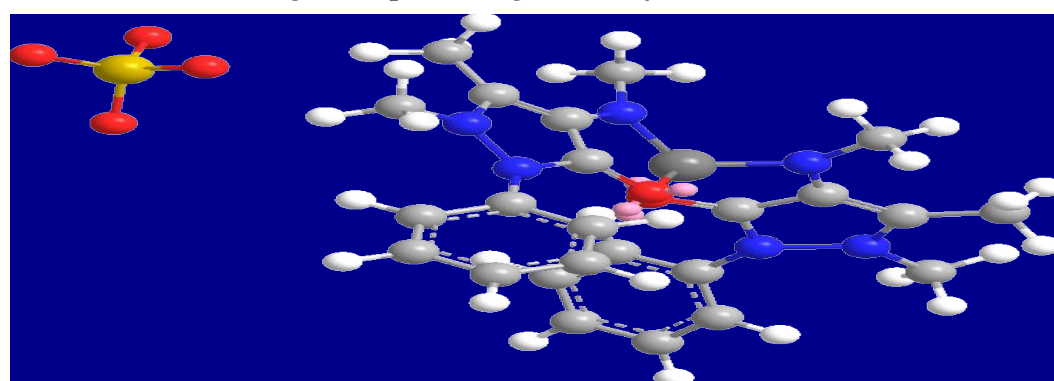


*Fig.(6): Optimized geometric for NiMAP.*

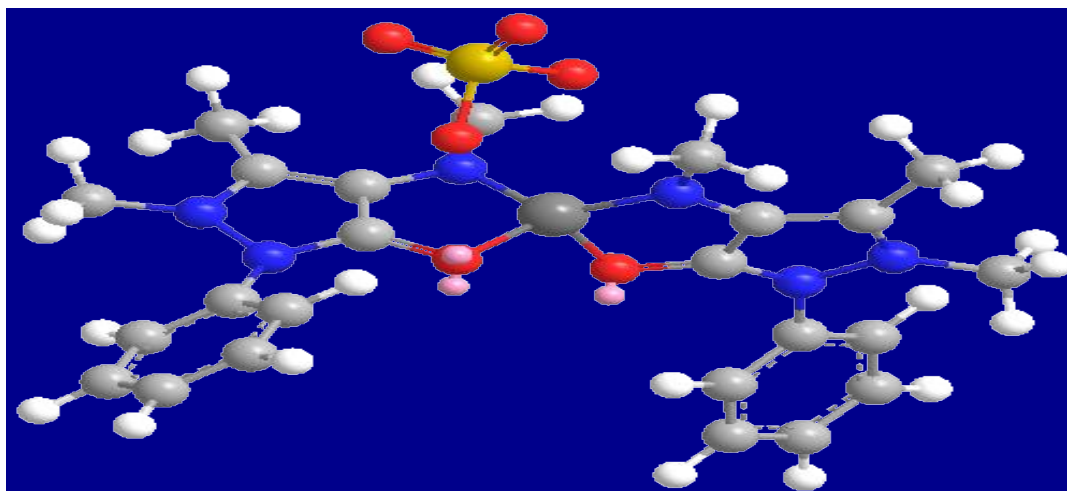
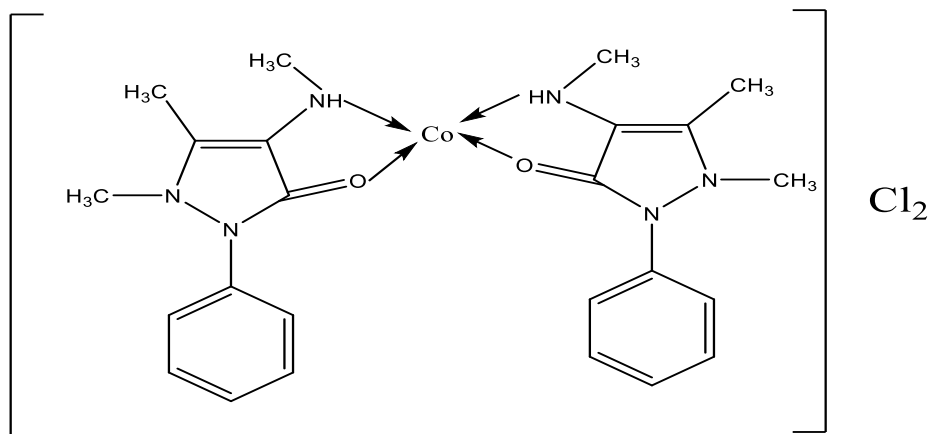


Fig.(7): Optimized geometric for CuMAP.

E.P	LUMO	HOMO	$\text{Ni}^{2+}$
			$\text{Ni}^{2+}$
			$\text{Co}^{2+}$
			$\text{Cu}^{2+}$

Fig.(8): Electrostatic potential, HOMO and LUMO for complexes.



Chemical Formula:  $C_{24}H_{30}Cl_2CoN_6O_2$

Exact Mass: 563.11

Molecular Weight: 564.37

m/z: 563.11 (100.0%), 565.11 (64.5%), 564.12 (26.4%), 566.11 (18.0%), 567.11 (10.6%), 565.12 (3.8%), 568.11 (3.0%), 567.12 (2.4%), 564.11 (2.2%)

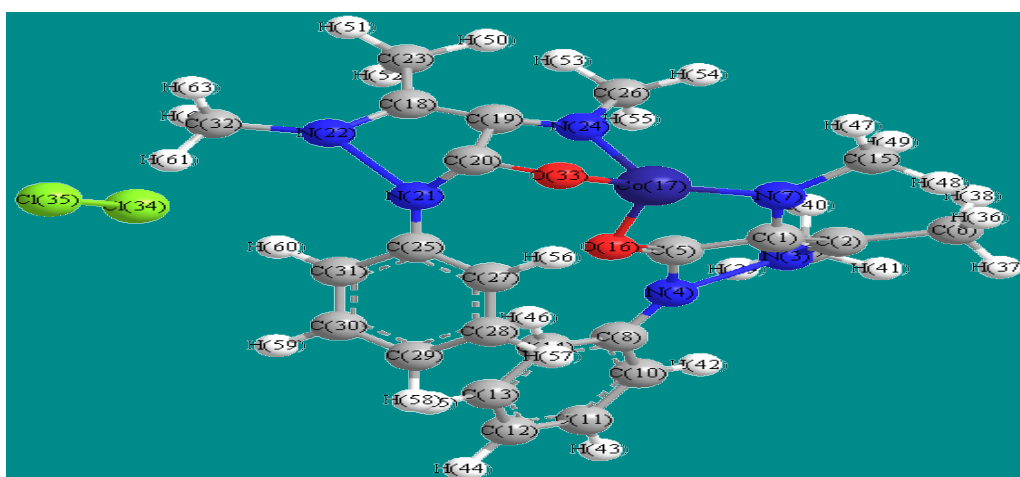


Fig.(9): Serial number of atoms of CoMAP.

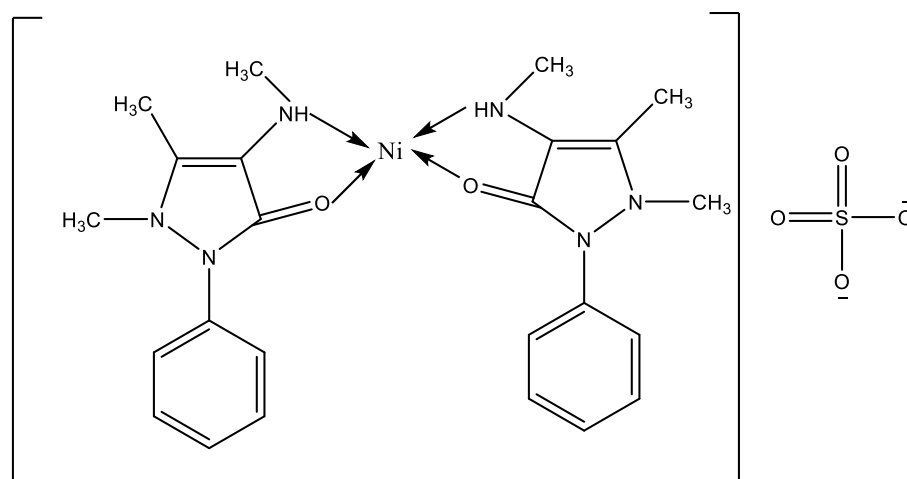
Table(7)

Selected molecular structure parameters of Bond lengths ( $\text{\AA}$ ) of CoMAP.

Atoms	Actual	optimal	Atoms	Actual	optimal	Atoms	Actual	optimal
C(32)-H(63)	1.113	1.113	C(34)-C(35)	1.398		N(21)-C(15)	1.366	1.462
C(32)-H(62)	1.113	1.113	Co(17)-O(16)	1.7934	1.45	C(19)-N(24)	1.366	1.462
C(32)-H(51)	1.113	1.113	O(33)-Co(17)	1.8596	1.45	C(18)-C(23)	1.497	1.497
C(31)-H(60)	1.1	1.1	N(7)-Co(17)	1.836		C(20)-N(21)	1.366	1.462
C(30)-H(59)	1.1	1.1	Co(17)-N(24)	1.836		N(21)-C(18)	1.366	1.462
C(19)-H(58)	1.1	1.1	C(20)-O(33)	1.333	1.333	N(21)-N(22)	1.3938	
C(18)-H(57)	1.1	1.1	N(22)-C(32)	1.47	1.47	C(19)-C(20)	1.337	1.368
C(32)-H(63)	1.113	1.113	C(31)-C(15)	1.337	1.42	C(18)-C(19)	1.337	1.337
C(20)-O(33)	1.333	1.333	C(30)-C(31)	1.337	1.42	C(3)-C(16)	1.333	1.333
N(21)-C(32)	1.47	1.47	C(29)-C(30)	1.337	1.42	N(7)-C(15)	1.47	1.47

**Table(8)**  
**Selected molecular structure parameters (Bond angle) of CoMAP.**

Atoms	Actual	optimal	Atoms	Actual	optimal	Atoms	Actual	optimal
C(30)- H(59)	1.1	1.1	Cl(34)- Cl(35)	1.98		N(24)- C(19)- C(20)	111	120
C(29)- H(58)	1.1	1.1	Co(17)- O(16)	1.7954	1.45	N(24)- C(19)- C(18)	120	120
C(28)- H(57)	1.1	1.1	O(33)- Co(17)	1.8596	1.45	C(20)- C(19)- C(18)	111	120
C(31)- H(60)	1.1	1.1	N(7)- Co(17)	1.836		C(23)- C(18)- N(22)	124.5	125.3
Cl(34)- Cl(35)	1.98		Co(17)- N(24)	1.836		C(23)- C(18)- C(19)	124.5	121.4
Co(17)- O(16)	1.7954	1.45	O(20)- O(33)- Co(17)	98.5759		N(22)- C(18)- C(19)	111	120
O(33)- Co(17)	1.8596	1.45	H(63)- C(32)- H(62)	109.52	109	O(33)- Co(17)- N(24)	83.2186	
N(7)- Co(17)	1.836		H(63)- C(32)- H(61)	109.4618	109	O(33)- Co(17)- O(16)	106.9214	
Co(17)- N(24)	1.836		H(63)- C(32)- N(22)	109.4618		O(33)- Co(17)- N(7)	159.0124	



Chemical Formula:  $C_{24}H_{30}N_6NiO_6S$

Exact Mass: 588.13

Molecular Weight: 589.29

m/z: 588.13 (100.0%), 590.13 (45.1%), 589.13 (29.2%), 591.13 (13.2%), 592.12 (7.1%), 590.14 (3.4%), 592.13 (2.8%), 593.13 (1.7%), 594.12 (1.7%), 591.12 (1.3%)

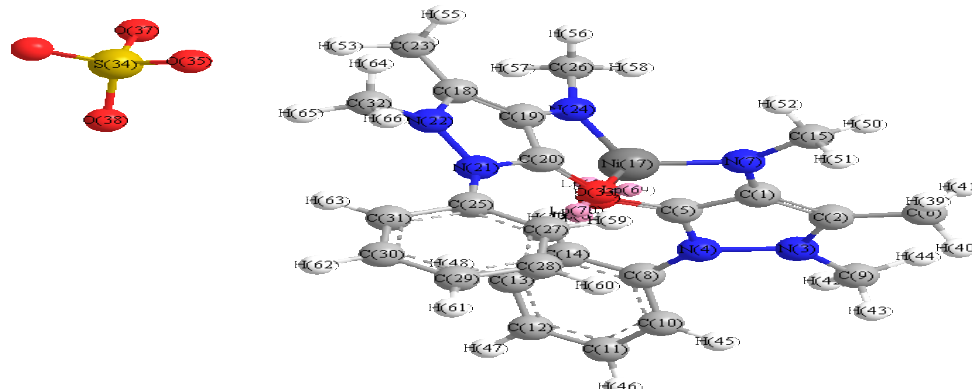


**Fig.(10): Serial number of atoms of NiMAP.**

**Table(9)**  
*Selected molecular structure parameters of Bond lengths (Å) for NiMAP.*

Atoms	Actual	optimal	Atoms	Actual	optimal	Atoms	Actual	optimal
O(33)- Lp(70)	0.5896	0.6	O(9)- H(44)	1.1125	1.113	C(19)- N(24)	1.3865	1.462
O(33)- Lp(69)	0.6001	0.6	O(9)- H(43)	1.1133	1.113	C(18)- C(23)	1.5014	1.497
O(16)- Lp(68)	0.6002	0.6	O(9)- H(42)	1.1128	1.113	C(20)- N(21)	1.3565	1.462
O(16)- Lp(67)	0.5896	0.6	N(17)- O(16)	1.7445		N(22)- C(18)	1.3708	1.462
O(32)- H(66)	1.1129	1.113	O(33)- N(17)	1.7456		N(21)- N(22)	1.4945	
O(32)- H(65)	1.1131	1.113	N(7)- N(17)	1.7636		C(19)- C(20)	1.4174	1.503
N(3)-C(9)	1.4715	1.47	N(17)- N(24)	1.7629		C(18)- C(19)	1.4024	1.537
N(4)-C(8)	1.467	1.462	C(5)-C(1)	1.4175	1.503	C(5)- O(16)	1.3685	1.355
N(7)- C(15)	1.4549	1.47	N(4)-C(5)	1.3577	1.462	C(27)- C(28)	1.3949	1.42
C(14)- C(8)	1.4057	1.42	C(1)-N(3)	1.3703	1.462	C(25)- C(27)	1.4058	1.42

**Table (10)**  
*Selected molecular structure parameters (Bond angle) of NiMAP.*

O(38)- S(34)- O(37)	108.0853		C(31)- C(25)- C(27)	118.5985	120	C(20)- C(19)- C(18)	111.2147	120
O(38)- S(34)- O(36)	108.1857		C(31)- C(25)- N(21)	119.9405	120	C(23)- C(18)- N(22)	128.6839	125.3
O(38)- S(34)- O(35)	108.135		C(27)- C(25)- N(21)	121.4204	120	C(23)- C(18)- C(19)	126.9047	121.4
O(36)- S(34)- O(35)	115.8429	116.6	C(28)- N(24)- C(19)	125.3383	108	N(22)- C(18)- C(19)	103.7385	120
Lp(70)- O(33)- Lp(69)	125.4626	131	C(26)- N(24)- Ni(17)	130.7335		O(33)- Ni(17)- N(24)	99.7292	
Lp(70)- O(33)- C(20)	105.4315	103.26	C(19)- N(24)- Ni(17)	108.7237	109	O(33)- Ni(17)- O(16)	111.7717	
C(32)- H(64)	1.1126	1.113	H(55)- C(23)- H(54)	108.9485	109	O(33)- Ni(17)- N(7)	113.5786	
C(31)- H(63)	1.1013	1.1	O(33)- C(20)- C(19)	121.5966	124.3	N(4)- N(3)- C(2)	110.9255	
C(30)- H(62)	1.1022	1.1	N(21)- C(20)- C(19)	108.1381	120	N(7)- C(1)- C(5)	113.3623	120
C(29)- H(61)	1.102	1.1	N(24)- C(19)- C(20)	113.3058	120	N(7)- C(1)- C(2)	135.2701	120

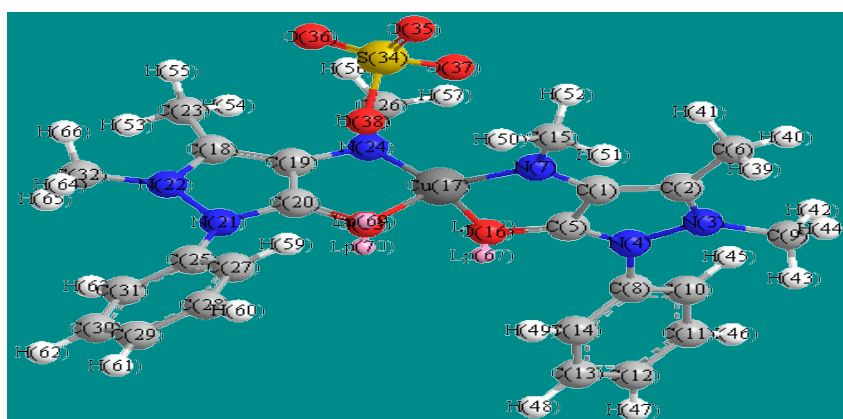
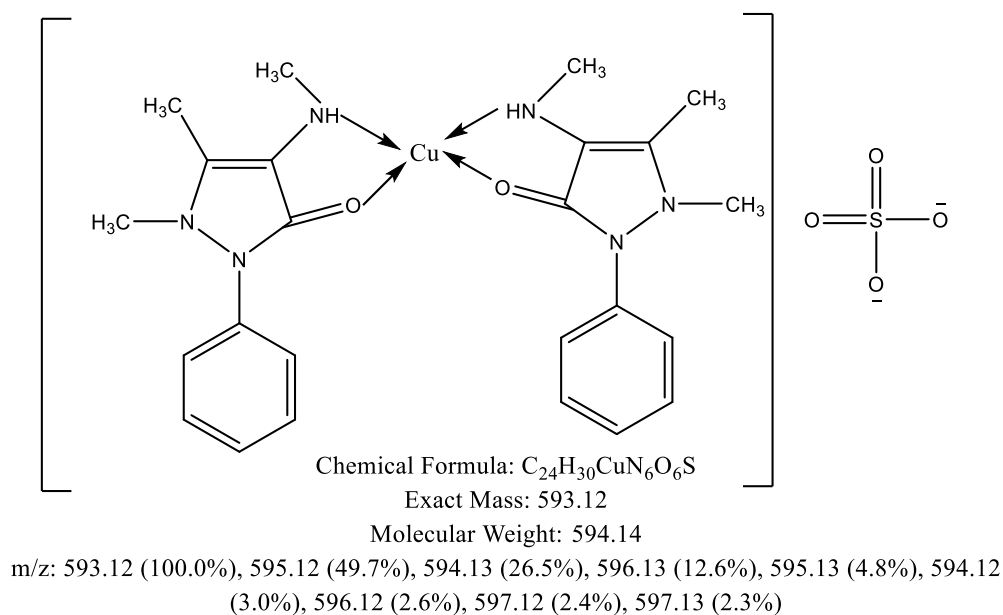


Fig.(11): Serial number of atoms of CuMAP.

Table (11)  
 Selected molecular structure parameters (Bond lengths, Å) of CuMAP

Atoms	Actual	optimal	Atoms	Actual	optimal	Atoms	Actual	optimal
O(33)-Lp(70)	0.5972	0.6	C(5)-C(1)	14122	1508	C(13)-C(14)	13946	1.42
O(33)-Lp(69)	0.6001	0.6	N(4)-C(5)	13559	1462	C(12)-C(13)	13969	1.42
O(16)-Lp(68)	0.6005	0.6	C(2)-N(3)	13702	1462	C(11)-C(12)	13987	1.42
O(16)-Lp(67)	0.5988	0.6	C(27)-H(59)	11005	11	C(10)-C(11)	13933	1.42
S(34)-O(36)	1.4496	1.45	C(26)-H(58)	11128	1113	C(9)-C(10)	14062	1.42
S(34)-O(35)	1.449	1.45	C(26)-H(57)	11127	1113	N(3)-C(9)	14714	1.47
O(16)-Cu(17)	1.8297		C(26)-H(56)	11123	1113	N(4)-C(8)	14413	1.462
N(7)-Cu(17)	1.8341		C(23)-H(55)	11134	1113	C(1)-N(7)	13867	1.462
N(24)-Cu(17)	1.8342		C(23)-H(54)	11093	1113	C(2)-C(6)	1501	1.497
O(33)-Cu(17)	1.8107		C(23)-H(53)	1113	1113	N(22)-C(32)	14721	1.47

**Table (12)**  
**Selected molecular structure parameters (Bond angle) of CuMAP.**

Atoms	Actual	optimal	Atoms	Actual	optimal	Atoms	Actual	optimal
O(35)- S(34)- O(35)	118.4972	115.5	N(21)- C(20)- C(19)	108.5702	120	N(24)-Cu(17)- O(16)	105.9545	
Lp(70)- O(33)- Lp(68)	118.3634	131	N(24)- C(19)- C(20)	112.7167	120	N(24)-Cu(17)- N(7)	130.9612	
Lp(70)- O(33)- C(20)	100.8591	103.25	N(24)- C(19)- C(18)	136.3091	120	O(16)-Cu(17)- N(7)	93.1362	
H(65)- C(31)- C(30)	119.0224	120	C(20)- C(19)- C(18)	110.9709	120	Lp(68)-O(16)- Lp(67)	121.0831	131
H(65)- C(31)- C(25)	120.1667	120	C(25)- C(18)- N(22)	128.3828	123.3	Lp(68)-O(16)- Cu(17)	116.3027	
H(65)- C(31)- C(30)	119.0224	120	H(45)- C(10)- C(11)	119.2016	120	Lp(68)-O(16)- C(5)	108.9855	103.25
C(18)- N(24)- Cu(17)	130.6428		H(45)- C(10)-C(8)	120.1486	120	N(24)-Cu(17)- O(16)	105.9545	
C(19)- N(24)- Cu(17)	105.8222		H(45)- C(10)- C(11)	119.2016	120	Cu(17)-O(16)- C(5)	108.7855	

## Conclusion

The theoretical study of Hyperchem 8.0.7 program using Semi-empirical calculations and PM3 method help to characterized MAP complexes by calculate optimized geometries, HOMO, LUMO, electrostatic potential and vibrational frequencies, these data are shown good agreement with the experimental data that which were used elemental and spectroscopic analysis. Chemoffice program used to draw the structure of MAP complexes and calculate the CHNOS analysis, also Chemoffice 3D used to draw 3D structure of molecules, bond distances and bond angles.

## Reference

- [1] Ergun H., Frattarelli D.A.C., Aranda J.V.J., "Characterization of the role of physicochemical factors on the hydrolysis of dipyrone", J. Pharm. Biomed. Anal., 35, 479-487, 2004.
- [2] Mario G., Virginia D. V., Hong K. L., Fulvio L., Cezary K., Vanessa F., Artur B., Cecilia V., "Pharmacokinetic investigations of the marker active metabolite-4-methylamino-antipyrin after intravenous and intramuscular injection of metamizole in healthy sheep", 132, 143-146, 2015.
- [3] Sigroha S., Narasimhan B., Kumar P., Khatkar A., Ramasamy K., Mani V., Mishra R. K., Abdul Majeed AB., "Design, Synthesis, Antimicrobial, Anticancer Evaluation, and QSAR studies of 4(substitutedbenzylidene-amino)-1,5-dimethyl-2-phenyl-1,2-dihydropyrazol-3-ones", Med. Chem. Res., 21(11), 3863-3875, 2012.
- [4] Teng Y., Liu R., Li C., Zhang H., "Effect of 4-aminoantipyrine on Oxidative Stress Induced by Glutathione Depletion in single Human Erythrocytes using a Micro Fluidic device together with Fluorescence Imaging", J Hazardous Materials, 192, 1766-1771, 2011.
- [5] Joseph J., Nagashri K., Ayisha Bibin Rani G., "Synthesis, characterization and antimicrobial activities of copper complexes derived from 4-aminoantipyrine derivatives", Journal of Saudi Chemical Society, 17(3), 285-294, 2013.
- [6] Salem O., Thabet H., Ashraf F. and Fathiya A., "Study on the relationship between genetic polymorphisms of cytochrome P450 and effects of Methylaminoantipyrine in dental pain", Journal of Chemical and Pharmaceutical Research, 8(4), 1365-1373, 2016.
- [7] Rezende R. M., França D. S., Menezes G. B., dos Reis W. G. P., Bakhle Y. S. and Francischi J. N., "Different mechanisms underlie the analgesic actions of paracetamol and dipyrone in a rat model of inflammatory pain", Br J Pharmacol., 153(4), 760-768, 2008.
- [8] Yi L., Yuanyuan L., Haowei W., Xiaohui X., Ping W. and Fangshi L., "Synthesis, Crystal Structure, Vibration Spectral, and DFT Studies of 4-Aminoantipyrine and Its Derivatives", Molecules, 18, 877-893, 2013.

- [9] Mostafa M. G., Marwa G. and Mansour S., "Synthesis, Characterization and Anti-Breast Cancer Activity of New 4-Aminoantipyrine-Based Heterocycles", *Int. J. Mol. Sci.*, 15, 7539-7553, 2014.
- [10] Abdullah M. and Salman A., "Synthesis and Anti-Bacterial Activities of Some Novel Schiff Bases Derived from Aminophenazone", *Molecules*, 15, 6850-6858, 2010.
- [11] Priti D., Pradeep K. S., Amit K., Anand K. H., Renu D., "4-Aminoantipyrine: A Significant Tool for the Synthesis of Biologically Active Schiff Bases and Metal Complexes", *Int. J. Pharm. Sci. Rev. Res.*, 34(1), 162-170, 2015.
- [12] Thamarai S., Mahalakshmi S., "Synthesis and Characterization of new Heterocyclic Schiff base ligand derived from 4-Amino Antipyrine", *International Journal of Advance Research and Development*, 2(2), 51-56, 2017.
- [13] Acha U. E., Olalere G. A., Opeyemi A. A., Nelson O., "Computational and Experimental Studies of 4-Aminoantipyrine as Corrosion Inhibitor for Mild Steel in Sulphuric Acid Solution", *Int. J. Electrochem. Sci.*, 7, 534-553, 2012 .
- [14] Robert M.S., Francis X.W., David J. K., David L.B., *Spectrometric Identification of Organic Compounds*, John Wiley and Sons, edition(8)<sup>th</sup>, 2015.
- [15] Rajasekar K. and Ramachandramoorthy T., "Synthesis, Spectral characterization and biological activities of Cr(III), Co(II), Ni(II) and Cd(II) complexes with 4-aminoantipyrineand thiocyanate ion as ligands", *Int J Pharm Bio Sci*, 4(2), 271 – 276, 2013.
- [16] Tudor R., Simona P., Veronica L., Carmen Ch. and Raluca C., "Copper (II) Complexes with Ligands Derived from 4-Amino-2,3-dimethyl-1-phenyl-3-pyrazolin-5-one: Synthesis and Biological Activity", *Molecules*, 11, 904-914, 2006 .
- [17] Aayad A.S., Hussain J.M., "Thermal Analysis of Different Pyrazolone Azo Derivative and Their Complexes with Pd(II), Ni(II) and Ag(I)", *International Journal of Science and Research (IJSR)*, 4 (6), 504-508, 2015.